

# Ductility and Strain Behaviour of Ultra-high Performance Fibre Reinforced Concrete Beam Containing Coarse Aggregate under Shear Load

Abutu Simon John Smith<sup>1</sup>, Wadslin Frenelus<sup>2</sup>, Shawon Msughter Caesar<sup>3</sup>

<sup>1</sup>Federal University of Technology, Babura, Nigeria  
Department of Civil Engineering  
[abutusmith@gmail.com](mailto:abutusmith@gmail.com)

<sup>2</sup>China Three Gorges University, Yichang, China  
College of Hydraulic and Environmental Engineering  
[wadslin@ctgu.edu.cn](mailto:wadslin@ctgu.edu.cn)

<sup>3</sup>Nigerian Building and Road Research Institute, Ota, Nigeria  
Building Research Department  
[shawoncaesar7@gmail.com](mailto:shawoncaesar7@gmail.com)

**Abstract** - In this present paper, four point loading configuration was used to assess the effect of steel fibre volume ( $V_f$ ), type of steel fibre, presence/absence of stirrup and shear span to depth ratio ( $a/d$ ) on the ductility and strain behaviour of the UHPFRC-CA beam. Findings from the study revealed that  $a/d$  has the most influence on the ductility of UHPFRC-CA beam as it favours the development of new cracks, propagation of existing cracks and the realization of high shear capacity.  $V_f$  of up to 2% improves UHPFRC-CA beam's ductility beyond which leads to ductility reduction. Shear reinforcement in form of stirrups does not have significant impact on the ductility of UHPFRC-CA beam. UHPFRC-CA beam has lower compressive strain and higher tensile strain than the compressive strain and tensile strain of its cube specimen and dogbone specimen respectively. The use of hooked-end steel fibre and increase in  $V_f$  from 2% to 3% in the beam resulted in strain reduction in the compression zone of the UHPFRC-CA beam. The strain in the tension zone of UHPFRC-CA beam increased with the use of hooked-end steel fibre, increase in  $V_f$  from 2% to 3%, exclusion of stirrups and decrease in  $a/d$  from 2.82 to 2.08. The shear zone of UHPFRC-CA beam is characterized with low strain growth rate from the appearance of diagonal crack to failure; and the shear zone of UHPFRC-CA beam experienced strain reduction with the use of hooked-end steel fibre and increase in  $V_f$  from 2% to 3%. Finally, findings from the ductility and strain behaviour of this UHPFRC-CA beams can be utilized during research design and experimental stages to forecast the crack pattern and failure mode of UHPFRC-CA beam in terms of concrete crushing.

**Keywords:** coarse aggregate, ductility, shear load, strain, ultra-high performance fibre reinforced concrete

## 1. Introduction

Can concrete beams reinforced with high strength longitudinal steels be both ultra-strong and remarkably ductile? Engineers often face a trade-off between strength and flexibility in structural design but the use of ultra-high-performance fibre reinforced concrete with coarse aggregate (UHPFRC-CA) has changed that narrative. However, questions remain about how to optimize materials to give UHPFRC-CA beam the best ductility and strain performance under real-world loads. The ductility property of UHPFRC-CA beam gives it the ability to resist deformation as it undergoes elastic and plastic phases of deformation before eventual failure. Studies [1, 2] have shown that ultra-high performance concrete (UHPC) without fibre is highly brittle, prompting researchers to solve UHPC brittleness problem with the use of fibres in UHPC [2]. Wille et al. [3] reported that the introduction of fibres in UHPC changed its mode of failure from brittle to ductile with strain hardening curve. Yan et al [4] in their study found that the ductility of UHPC was improved with fibre addition as it altered the crack path due to the increased crack length. Bae et al. [5] investigated the correlation between ductility and tensile strength of ultra-high performance fibre reinforced concrete (UHPFRC) and findings revealed that while increased steel fibre volume in UHPC leads to increase in ductility, increase in tensile strength leads to decrease in

ductility. Fracture energy of UHPFRC has direct correlation to its ductility as increase in fracture energy due to increased volume of glass fibre leads to increase in ductility [6]. It was reported that the anchorage pattern involving the external bonding of carbon fibre reinforced polymer in UHPC leads to improvement in its flexural ductility [7]. In a study involving the ductility and flexural toughness of UHPFRC beams under bending load, Yang et al. [8] explained that the inclusion of steel fibre volume up to 1.5% in UHPC led to increased ductility but the use of 2.0% volume of steel fibre did not lead to any significant increase in the beams' ductility.

The high tensile strength of UHPFRC allows its beam to resist cracking even when the beam experiences large strains beyond 0.0025, making it to exhibit a strain-hardening behaviour [9]. The strains in UHPFRC beams are usually evaluated using internet of things (IOTs) sensors like strain gauge or displacement gauge; and then illustrated graphically through strain profiles [10]. Hussein [10] in his study discovered that the development of cracks around the vicinity of a strain gauge usually lead to increase in strain on the UHPFRC member. Strain gauges attached to the extreme compression and tension fibres of UHPFRC beams subjected to flexural loading are usually used to study its strain behaviour; while for beams subjected to shear loading, strain gauges attached to the shear zone where inclined cracks occur are used for investigating their strain behaviour [11].

So far, research delving deep into the study of the ductility and strain behaviours of UHPFRC structural members has been very limited, with research focus usually directed towards mechanical and other structural performances. For ultra high performance fibre reinforced concrete beams containing coarse aggregate (UHPFRC-CA), literature on the ductility and strain behaviour of such beams under flexural or shear loading is rare to find, despite the importance of understanding ductility and strain profiles in UHPFRC/UHPFRC-CA beams' experimental procedures. This study therefore aims to evaluate the effect of steel fibre volume ( $V_f$ ), type of steel fibre, presence/absence of stirrup and shear span to depth ratio ( $a/d$ ) on the ductility and strain behaviour of UHPFRC-CA beam under shear loading. This research will as well equip Engineers with practical strategies to design UHPFRC-CA beams that balances strength and ductility, paving the way for safer and more durable structures.

## 2. Experimental Methods

The materials presented in Table 1 were used for this study and Funk and Dinger [12] model presented in Eq. (1) was used to design the two UHPFRC-CA mixes, with one containing 2% volume of straight steel fibre and the other containing 3% volume of straight steel fibre.

$$P(D) = 100 \times \frac{D^q - D_{min}^q}{D_{max}^q - D_{min}^q} \quad (1)$$

where  $P(D)$  is the volume fraction of the total solids smaller than size  $D$ ,  $D$  is the particle size,  $D_{max}$  is the optimum particle size,  $D_{min}$  is the smallest particle size,  $q$  is the distribution modulus.

Table 1: Mix ratio of the UHPFRC-CA

Materials	UHPFRC-CA (2% vol.)	UHPFRC-CA (3% vol.)
P.O 52.5 Cement	1	1
P.C 42.5 Cement	0.6999	0.6999
Quartz sand ( $\leq 1$ mm)	1.9999	1.9999
Gravel (5-10mm)	0.8948	0.8948
Silica fume	0.2999	0.2999
Steel fibres	0.2895	0.4387
Super plasticizer	0.0488	0.0488
Water	0.3606	0.3606

The UHPFRC-CA beam presented in Figure 1 was designed based on EN 1992-1-1 [13], BS 8110-1 [14], Merchand [15] and Narayanan and Darwish [16] to have 1200mm length, 200mm height, 100mm breadth, 15mm

cover, 0.0373 longitudinal reinforcement ratio ( $\rho$ ), 2 $\Phi$ 20 high strength tensile reinforcement steel, 2 $\Phi$ 6.5 high strength compressive reinforcement steel and  $\Phi$ 6.5 high strength shear reinforcement steel.

Five beam specimens with the following descriptions as presented in Table 2 were tested for ductility and strains under four point loading configuration [17]: ASS-2-2.82 represents Beam A with straight steel fibre, stirrup, 2% volume of fibres and  $a/d$  of 2.82 (taken as the control beam). AHS-2-2.82 represents Beam A with hooked-end steel fibre, with stirrups, 2% vol. of fibres and  $a/d$  of 2.82. ASS-3-2.82 represents Beam A with straight steel fibre, stirrup, 3% vol. of fibres and  $a/d$  of 2.82. ASS<sub>w</sub>-3-2.82 represents Beam A with straight steel fibre, 3% vol. of fibres,  $a/d$  of 2.82 and without stirrups. ASS-2-2.08 represents Beam A with straight steel fibre, with stirrups, 2% vol. of fibres and  $a/d$  of 2.08.

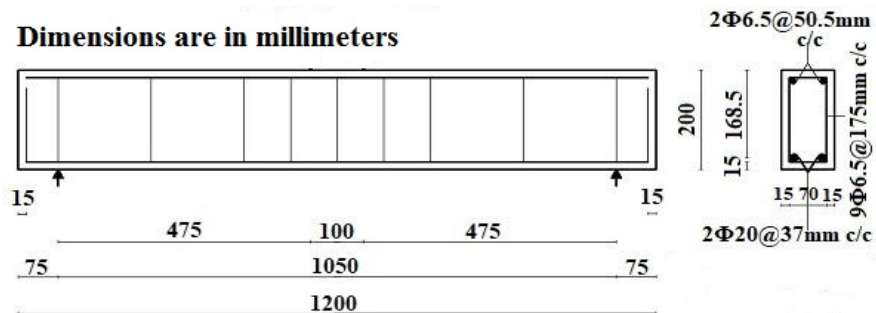


Fig. 1: Beam's longitudinal-cross section

Table 2: Beam specimens with research parameters

Beam specimen	Steel fibre	$V_f$ (%)	Stirrups	$a/d$
ASS-2-2.82	Straight	2	Yes	2.82
AHS-2-2.82	Hooked-end	2	Yes	2.82
ASS-3-2.82	Straight	3	Yes	2.82
ASS <sub>w</sub> -2-2.82	Straight	2	No	2.82
ASS-2-2.08	Straight	2	Yes	2.08

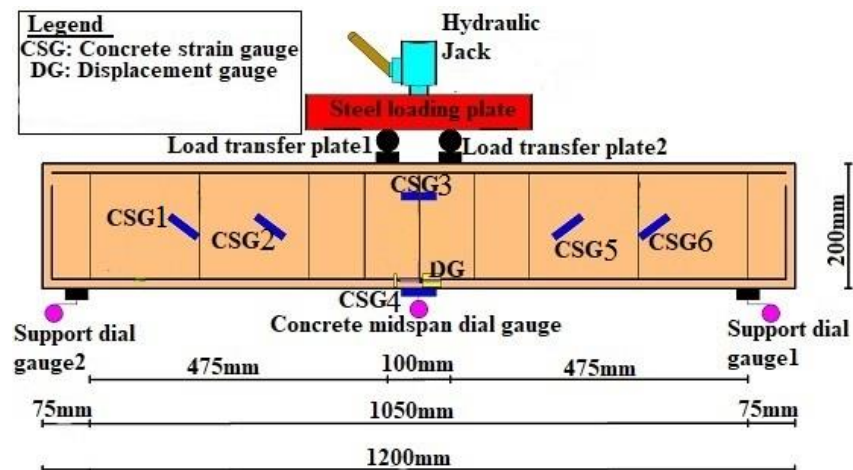


Fig. 2: Beam's set up

Strain gauges were attached to the beams to study their strain behaviour and dial gauges were attached to the beams to help in their ductility evaluation (as illustrated in Figure 2) using the following equation [18]:

$$\mu_u = \frac{\Delta_u}{\Delta_y} \quad (2)$$

where  $\mu_u$  is the deflection ductility index,  $\Delta_u$  is the deflection at the ultimate load and  $\Delta_y$  is the deflection at yielding of tensile steel reinforcement.

CSG1, CSG2, CSG 5 and CSG6 are concrete strains in the beams' shear zone; while CSG3 and CSG4 are the concrete strains around the beams' compression zone and tension zone respectively.

### 3. Results and Discussions

#### 3.1 Ductility of the UHPFRC-CA Beams

The ductility of the beams as presented in Figure 3 showed that ASS-2-2.82, AHS-2-2.82, ASS-3-2.82, ASS<sub>w</sub>-2-2.82, ASS-2-2.08 have ductility index of 1.54, 1.3, 1.41, 1.49, 1.79 respectively. These beams, even with their low ductility indices, can be said to have better ductility than some high performance concrete and reinforced concrete beams reported in other studies [19-21]. ASS-2-2.08 has better ductility performance than all the other beams and this is due to the reduced  $a/d$  value. This better ductility performance for ASS-2-2.08 means that it has the capability of absorbing high fracture energy; the property which favours the development of new cracks, propagation of existing cracks and the realization of high shear capacity. This better ductility performance allowed ASS-2-2.08 to undergo pure shear failure with double diagonal cracks as reported in Smith and Xu [22].

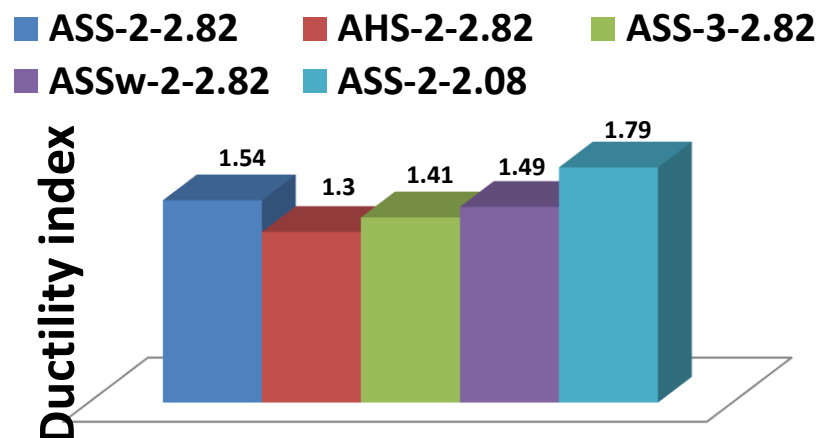


Fig. 3: Ductility of the beams

The ductility indices of the beams can also be comparable with the ductility indices of some UHPFRC beams having similar longitudinal reinforcement ratios and subjected to the same loading conditions reported by other researchers [18, 23]. These UHPFRC-CA beams exhibit low ductility indices because they were all reinforced with high strength steels in their tensile zones; which in turn have high yield strengths [24]. By implication, these steels yield at high applied loads resulting in high deflection values that have no serious difference with the deflection at ultimate loads. So this high deflection at yielding of steel reinforcement eventually leads to low ductility of the beams. The beams' low ultimate strains in the compression fibre also have direct impact on their low ductility indices.

In terms of the influence of the various research parameters on the UHPFRC-CA beam's ductility and their corresponding ultimate load and crack width, Figure 3 showed that the beam with straight steel fibre (ASS-2-2.82) has better ductility than the beam made with hooked-end steel fibre (AHS-2-2.82) as its ductility index decreased by about 16% when hooked-end steel fibre was used. Table 3 showed that ASS-2-2.82 has a lower crack width (1.4mm) than

AHS-2-2.82 (1.6) at the ultimate load of 273kN and 258kN respectively in which the ductility indices were estimated. The analysis of the beams revealed that increase in percentage volume of steel fibre from 2% (ASS-2-2.82) to 3% (ASS-3-2.82) reduced the beam's ductility by 8%; meaning that higher percentage volume of straight steel fibre beyond 2% does not improve the ductility of UHPFRC-CA beam; and Table 3 also revealed that ASS-3-2.82 has a wider crack (1.8mm) at ultimate load of 283kN than ASS-2-2.82's crack width of 1.4mm at 273kN. More so, the reduction in ductility of the beam with higher percentage volume of steel fibre was probably because the increased steel fibre contributed to the reduction in deflection of the beam at ultimate load phase. Further analysis of Figure 3 showed that the exclusion of stirrup reinforcement from ASS-2-2.82 to produce ASS<sub>w</sub>-2-2.82 does not lead to any significant decrease (only about 3% reduction) in the ductility of the beam; and this proved that stirrup contribution to UHPFRC-CA beam's ductility is almost insignificant. Table 3 also revealed that ASS<sub>w</sub>-2-2.82 has a higher crack width (2.9mm) than ASS-2-2.82 at the ultimate load of 265kN in which the ductility was evaluated. In addition, Figure 3 illustrated that decrease in *a/d* from 2.82 (ASS-2-2.82) to 2.08 (ASS-2-2.08) resulted in 16% increase in the beam's ductility with corresponding crack width of 3.6mm and ultimate load of 360kN as presented in Table 3.

**Table 3: Ultimate load and crack width corresponding to the UHPFRC-CA beam's ductility**

UHPFRC-CA Beam type	Load (kN)	Ductility	Crack width (mm)
ASS-2-2.82	273	1.54	1.4
AHS-2-2.82	258	1.3	1.6
ASS-3-2.82	283	1.41	1.8
ASS <sub>w</sub> -2-2.82	265	1.49	2.9
ASS-2-2.08	360	1.79	3.6

### 3.2 Load-Strain Relationship of the UHPFRC-CA Beams

CSG3 and CSG4 were respectively used to study the compressive strain and tensile strain of the beams; while the average of either CSG1 and CSG2 or CSG5 and CSG6 was used to investigate the inclined strains in the beams' shear zone where diagonal cracks developed and caused shear failure of the beams. So the load-strain relationship of the beams is discussed based on its location in the UHPFRC-CA beam and material (i.e. compression zone (CSG3), tensile zone (CSG4), shear zone (CSG1/CSG2 or CSG5/CSG6)).

#### 3.2.1 Strains in the UHPFRC-CA Beams' Compression Zone

ASS-2-2.82's CSG3 as presented in Figure 4 exhibited linear behaviour with its value at shear cracking load and ultimate load as 0.00043 and 0.0019 respectively. The compressive strain of ASS-2-2.82 was 27% lower than the ultimate strain from compressive strength test [25]; and this lower compressive strain may be the reason why there was no concrete crushing of the beam at failure. CSG3 of AHS-2-2.82 increased non-linearly with increase in the applied load and its value at shear cracking load and ultimate load was 0.00027 and 0.0015 respectively. This AHS-2-2.82's strain was 21% lower than that of ASS-2-2.82 at ultimate load phase and 46% lower than the ultimate strain from compressive strength test [25]. CSG3 of ASS-3-2.82 shown in Figure 4 increased non-linearly with increase in the applied load up to a load of 242kN with shear cracking load and ultimate load of 0.000033 and 0.0018 respectively; and it was 5% lower than that of ASS-2-2.82 at ultimate load phase and 49% lower than the ultimate strain from compressive strength test [25]. ASS<sub>w</sub>-2-2.82's CSG3 increased linearly with increase in the applied load with strains of 0.000033 and 0.0025 at shear cracking load and ultimate load respectively; and its value was 32% higher than that of ASS-2-2.82 at ultimate load phase and 3.8% lower than the ultimate strain from compressive strength test [25]. This increment between ASS-2-2.82 and ASS<sub>w</sub>-2-2.82 was as a result of the absence of stirrups which subjected the concrete to bear more load. The CSG3 of ASS-2-2.08 shown in Figure 4 also increased non-linearly with increase in the applied load and its value at shear cracking load and ultimate load was 0.00028 and 0.0021 respectively. This ASS-2-2.08's CSG3 was 11% higher than that of ASS-2-2.82 at ultimate load phase and 19% lower than the ultimate strain from compressive strength test [25]. This increase in strain between ASS-2-

2.82 and ASS-2-2.08 may be due to the increased number of cracks formed within the flexural zone of the beam where the strain gauges were located.

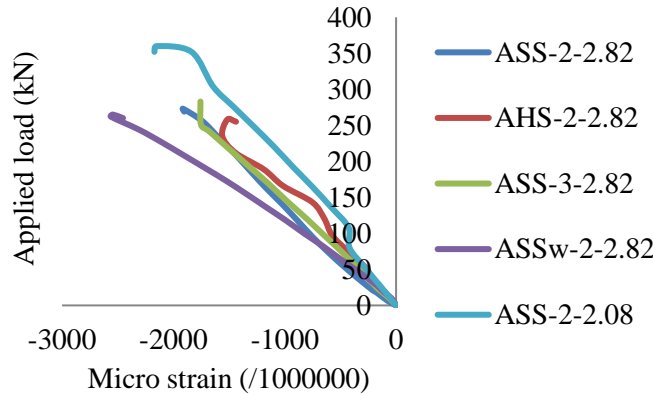


Fig. 4: Load-strain relationships of the beams in compression zone

### 3.2.2 Strains in the UHPFRC-CA Beams' Tension Zone

ASS-2-2.82's CSG4 based on Figure 5 was linear up to the load of 233kN and has the value of 0.0047, after which it became non-linear. At shear cracking load and ultimate load, the beam has a strain of 0.00078 and 0.0051 respectively. The tensile strain at ultimate load was about 47% higher than the ultimate strain from direct tensile test; and this higher strain may be due to localized effect resulting from the development of cracks within the tensile zone of the beam. CSG4 of AHS-2-2.82 based on Figure 5 only exhibited linear increment up to the cracking load of 28kN with a strain value of 0.00035, after which it became non-linear.

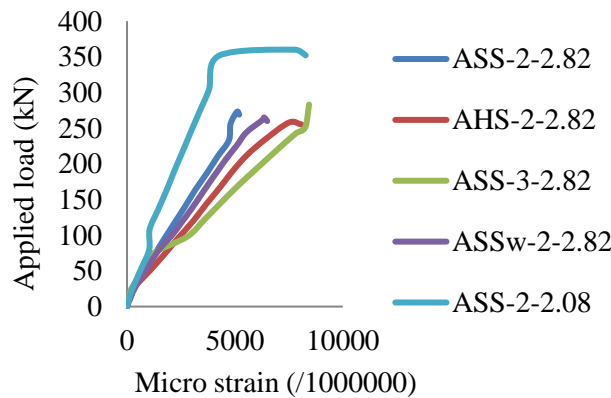


Fig. 5: Load-strain relationships of the beams in tension zone

AHS-2-2.82's CSG4 at shear cracking load and ultimate load phase were 0.0011 and 0.0081 respectively; and these strain values were higher than the shear cracking strain and ultimate strain of ASS-2-2.82 by 41% and 59% respectively. Figure 5 also showed that the ASS-3-2.82's CSG4 increased non-linearly with increase in applied load and has a value of 0.000072 and 0.0084 at shear cracking load and ultimate load respectively. Figure 5 further showed that CSG4 of ASS<sub>w</sub>-2-2.82 increased non-linearly with increase in applied load and has a value of 0.000076 and 0.0064 at shear cracking load and ultimate load respectively. ASS<sub>w</sub>-2-2.82's CSG4 was 25% higher than that of ASS-2-2.82 at ultimate load phase; and this increment was caused by the absence of stirrups which subjected the concrete to bear more load. CSG4 of ASS-2-2.08 based on Figure 5 exhibited non-linear increment on increment of the applied load with shear cracking strain and ultimate strain of 0.00064 and 0.0078 respectively; and this strain value at ultimate

load phase has shown that lower  $a/d$  ratio in the beam leads to 53% strain increase in the beam. The reason for the 53% increment may be due to the increased number of cracks formed within the flexural zone of the beam where the strain gauges were located.

### 3.2.3 Strains in the UHPFRC-CA Beams' Shear Zone

ASS-2-2.82's CSG1/CSG2 as shown in Figure 6 was only linear up to the first crack load of 28kN with a low strain value of 0.0000265. Beyond the cracking load, CSG1/CSG2 was non-linear until the failure load of the beam; and the strain at ultimate load was 0.0014. The non-linear behaviour of the shear zone's strain may be due to the change in direction and the stop in growth and propagation of some existing micro diagonal cracks near CSG1/CSG2. The development of shear failure mechanism of beam ASS-2-2.82 as studied through the growth of CSG1/CSG2 showed that although the rate of CSG1/CSG2 growth was not constant after the appearance of the main diagonal crack, there was no sudden and high increase in growth rate before failure of the beam; and the maximum strain growth rate was 0.00027. The CSG1/CSG2 of AHS-2-2.82 as shown in Figure 6 increased non-linearly with increase in applied load; and it has shear cracking strain and ultimate strain of 0.000011 and 0.0012 respectively. The CSG1/CSG2 of ASS-3-2.82 shown in Figure 6 has shear cracking strain and ultimate strain of 0.0000052 and 0.00088 (about 37% decrease when compared with ASS-2-2.82) respectively; and the 37% decrease in strain is due to the higher resistance to deformation provided by the increased percentage volume of steel fibre. The result of ASS<sub>w</sub>-2-2.82's CSG1/CSG2 shown in Figure 6 revealed that it has shear cracking strain and ultimate strain of 0.0000092 and 0.0016 (about 14% higher than ASS-2-2.82 at ultimate load phase) respectively; and the 14% increase is due to the multiple diagonal cracks formed around CSG1/CSG2. The analysis of Figure 6 showed that ASS-2-2.08's CSG1/CSG2 or CSG5/CSG6 increased non-linearly with increase in applied load and was broken by diagonal cracks at a strain and load value of 0.00098 and 164kN respectively. The strain of ASS-2-2.08 at shear cracking strain was 0.00012.

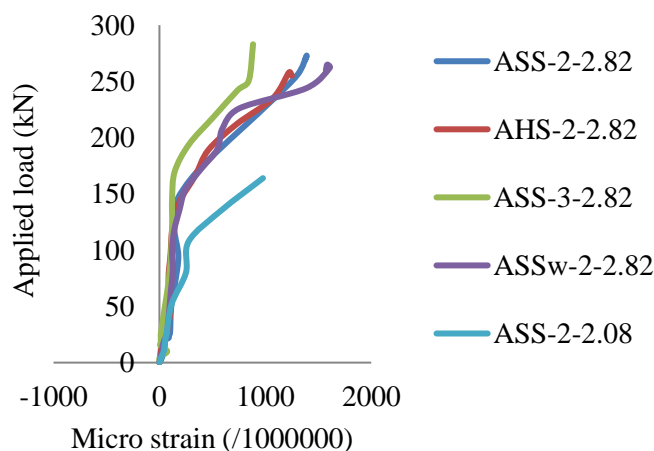


Fig. 6: Load-strain relationships of the beams in shear zone

## 4. Conclusion

This study investigates the ductility and strain properties of UHPFRC-CA beam subjected to shear loading using  $V_f$ , type of steel fibre, presence/absence of stirrup and  $a/d$  as research parameters. The following conclusions were drawn from the study:

The ductility of UHPFRC-CA beam is most influenced by  $a/d$  which favours new cracks formation, propagation of existing cracks and the realization of high shear capacity. The optimum  $V_f$  that improves UHPFRC-CA beam's ductility is 2%; and shear reinforcement in form of stirrups does not have significant impact on the ductility of UHPFRC-CA beam.

UHPFRC-CA beam has lower compressive strain and higher tensile strain when compared with the compressive strain and tensile strain of its cube specimen and dogbone specimen respectively. At the compression zone of UHPFRC-CA beam, the use of hooked-end steel fibre and increase in  $V_f$  from 2% to 3% in the beam cause strain reduction in the beam;

while the exclusion of stirrups and decrease in  $a/d$  from 2.82 to 2.08 cause strain increment in the beam. The use of hooked-end steel fibre, increase in  $V_f$  from 2% to 3%, exclusion of stirrups and decrease in  $a/d$  from 2.82 to 2.08 in UHPFRC-CA beam cause strain increment in its tension zone.

UHPFRC-CA beam exhibits low strain growth rate in its shear zone after diagonal crack appearance until failure. The strain in the shear zone of UHPFRC-CA beam undergo reduction with the use of hooked-end steel fibre and increase in  $V_f$  from 2% to 3%; while the exclusion of stirrups and decrease in  $a/d$  from 2.82 to 2.08 cause strain increment in the beam's shear zone.

Findings from the ductility of this UHPFRC-CA beams can be utilized during research design stage to forecast the crack pattern of its beam subjected to flexural or shear loading. The findings obtained from the strain behaviour of this study's beams are vital during flexural or shear strength experiment as they determined the failure mode of the UHPFRC-CA beam in terms of concrete crushing.

## References

- [1] J. Yang, G. F. Peng, Y. X. Gao, H. Zhang, "Mechanical properties and durability of ultra-high performance concrete incorporating coarse aggregate," *Key Engineering Materials*, vols. 629-630, no. 2014, pp. 96-103, 2014, <https://doi.org/10.4028/www.scientific.net/KEM.629-630.96>
- [2] Z. Wu, K. H. Khayat, C. Shi, "How do fibre shape and matrix composition affect fibre pullout behaviour and flexural properties of UHPC?," *Cement and Concrete Composite*, vol. 90, no. 2018, pp. 193-201, 2018, <https://doi.org/10.1016/j.cemconcomp.2018.03.021>
- [3] K. Wille, A. E. Naaman, S. El-Tawil, G. J. Parra-Montesinos, "Ultra-high performance concrete and fibre reinforced concrete: achieving strength and ductility without heat curing," *Materials and Structures*, vol. 45, no. 3, pp. 309-324, 2012, <https://doi.org/10.1617/s11527-011-9767-0>
- [4] P. Yan, B. Chen, S. Afgan, M. A. Haque, M. Wu, J. Han, "Experimental research on ductility enhancement of ultra-high performance concrete incorporation with basalt fibre, polypropylene fibre and glass fibre," *Construction and Building Materials*, vol. 279, no. 122489, pp. 1-15, 2021, <https://doi.org/10.1016/j.conbuildmat.2021.122489>
- [5] B. I. Bae, H. K. Choi, C. S. Choi, "Ductility of ultra-high performance concrete and its correlation with tensile strength increase," *Key Engineering Materials*, vol. 665, pp. 21-24, 2016, <https://doi.org/10.4028/www.scientific.net/KEM.665.21>
- [6] B. H. Mohammed, A. F. H. Sherwani, R. H. Faraj, H. H. Qadir, K. H. Younis, "Mechanical properties and ductility behaviour of ultra-high performance fibre reinforced concretes: Effect of low water-to-binder ratios and micro glass fibres," *Ain Shams Engineering Journal*, vol. 12, no. 2, pp. 1557-1567, 2021, <https://doi.org/10.1016/j.asej.2020.11.008>
- [7] H. K. S. El-Din, M. M. Husain, M. A. Khater, "Strength and ductility of ultra-high performance fibre reinforced concrete beams with externally cfrp sheets," *Egyptian International Journal of Engineering Sciences and Technology*, vol. 16, no. 1, pp. 46-58, 2013, <http://dx.doi.org/10.21608/eijest.2013.96791>
- [8] I. H. Yang, J. Park, T. Q. Bui, K. C. Kim, C. Joh, H. Lee, "An Experimental Study on the Ductility and Flexural Toughness of Ultrahigh-Performance Concrete Beams Subjected to Bending," *Materials*, vol. 12, no. 10, pp. 1-22, 2020, <https://doi.org/10.3390/ma13102225>
- [9] R. G. El-Helou, B. A. Graybeal, "Flexural behaviour and design of ultrahigh-performance concrete beams," *Journal of Structural Engineering*, vol. 148, no. 4, pp. , 2022, [https://doi.org/10.1061/\(ASCE\)ST.1943-541X.0003246](https://doi.org/10.1061/(ASCE)ST.1943-541X.0003246)
- [10] L. Hussein, "Structural behaviour of ultra-high performance fibre reinforced concrete composite members," PhD dissertation, Department of Civil Engineering, Ryerson University, Toronto, Canada, 2015.
- [11] B. A. Graybeal, "Structural behaviour of ultra-high performance concrete prestressed i-girders," FHWA-HRT-06-115, McLean, VA 22101-2296, 2006.

- [12] J. E. Funk, D. R. Dinger, "Predictive process control of crowded particulate suspensions, applied to ceramic manufacturing," Boston, U.S.A.: Kluwer Academic Publishers, 1994.
- [13] EN 1992-1-1, "Design of concrete structures-part 1-1: general rules and rules for buildings," Brussel: European Committee for Standardization (Eurocode), 2004.
- [14] BS 8110-1, "Structural use of concrete-part 1: code of practice for design and construction," London, United Kingdom: British Standard Institution, 1997.
- [15] P. Marchand, "New AFGC recommendations on UHPFRC: chapter 2-design," in *Designing and Building with UHPFRC-State-of-the-art-and-development*, F. Tootlemonde, J. Resplendino Eds. France: Wiley, 2009, pp. 743-754.
- [16] R. Narayanan, I. Y. S. Darwish, "Use of steel fibre as shear reinforcement," *ACI Structural Journal*, vol. 84, no. 3, pp. 216-227, 1987.
- [17] GB/T 50152, "Standard for test methods for concrete structures," Beijing, China: National Standard of the People's Republic of China, 2012.
- [18] I. H. Yang, C. Joh, B. S. Kim, "Structural behaviour of ultra-high performance concrete beams subjected to bending," *Engineering Structures*, vol. 32, pp. 3478-3487, 2010.
- [19] M. S. Islam, "Shear capacity and flexural ductility of reinforced high-and normal strength concrete beams," M.Phil thesis, Department of Civil Engineering, University of Hong Kong, 1996.
- [20] T. K. Kim, J. S. Park, "Evaluation of the performance and ductility index of concrete structures using advanced composite material strengthening methods," *Polymers*, vol. 13 no. 4239, pp. 1-10, 2021.
- [21] L. F. A. Bernardo, S. M. R. Lopez, "Neutral axis depth versus flexural ductility in high strength concrete beams," *Journal of Structural Engineering*, vol. 130, pp. 452-459, 2004.
- [22] A. S. J. Smith, G. Xu, "Influence of key shear factors on the shear performance of ultra-high performance fibre reinforced concrete beam containing coarse aggregate," *Periodica Polytechnica Civil Engineering*, vol. 68, no. 4, pp. 1378-1392, 2024, <https://doi.org/10.3311/PPci.36817>
- [23] V. Kodur, R. Solhmirzaei, A. Agrawal, E. M. Aziz, P. Soroushian, "Analysis of flexural and shear resistance of ultra-high performance fibre reinforced concrete beams without stirrups," *Engineering Structures*, vol. 174, pp. 873-884, 2018.
- [24] S. K. Baduge, P. Mendis, T. D. Ngo, M. Sofi, "Ductility design of reinforced very-high strength concrete columns (100-150MPa) using curvature and energy-based ductility indices," *International Journal of Concrete Structures and Materials*, vol. 13 no. 37, pp. 1-23, 2019.
- [25] A. S. J. Smith, "Shear behaviour of ultra-high performance fibre reinforced concrete beam containing coarse aggregate (UHPFRC-CA)," PhD thesis, College of Civil Engineering and Architecture, China Three Gorges University, Yichang, China, 2023.